Neuron, Vol. 43, 623–631, September 2, 2004, Copyright ©2004 by Cell Press

Clinical Study

Neural Basis of Genetically Determined Visuospatial Construction Deficit in Williams Syndrome

Andreas Meyer-Lindenberg,[1,*] Philip Kohn,[1] Carolyn B. Mervis,[2] J. Shane Kippenhan,[1] Rosanna K. Olsen,[1] Colleen A. Morris,[3] and Karen Faith Berman[1]

[1]Unit on Integrative Neuroimaging
Clinical Brain Disorders Branch
National Institute of Mental Health
National Institutes of Health
Department of Health and Human Services
10-4C101
9000 Rockville Pike
Bethesda, Maryland 20892

[2]Neurodevelopmental Sciences Laboratory
Department of Psychological and Brain Sciences
University of Louisville
Louisville, Kentucky 40292

[3]Department of Pediatrics
University of Nevada School of Medicine
University of Nevada
Las Vegas, Nevada 89102

Summary

A unique opportunity to understand genetic determinants of cognition is offered by Williams syndrome (WS), a well-characterized hemideletion on chromosome 7q11.23 that causes extreme, specific weakness in visuospatial construction (the ability to visualize an object as a set of parts or construct a replica). Using multimodal neuroimaging, we identified a neural mechanism underlying the WS visuoconstructive deficit. Hierarchical assessment of visual processing with fMRI showed isolated hypoactivation in WS in the parietal portion of the dorsal stream. In the immediately adjacent parietooccipital/intraparietal sulcus, structural neuroimaging showed a gray matter volume reduction in participants with WS. Path analysis demonstrated that the functional abnormalities could be attributed to impaired input from this structurally altered region. Our observations confirm a longstanding hypothesis about dorsal stream dysfunction in WS, demonstrate effects of a localized abnormality on visual information processing in humans, and define a systems-level phenotype for mapping genetic determinants of visuoconstructive function.

Introduction

Williams syndrome (WS) is caused by a hemizygous deletion of approximately 1.6 Mb on chromosome 7q11.23, including about 21 genes (Hillier et al., 2003). Disturbed visuospatial construction is a hallmark of the disorder (Frangiskakis et al., 1996), and individuals with WS have marked difficulty in tasks requiring the use of a pattern or object assembly (e.g., following a pattern to build a model or assembling a simple piece of furniture). WS is also characterized by dysmorphic features, mental retardation or learning difficulties, elastin arteriopathy, and a typical personality that includes overfriendliness and anxiety (Mervis and Klein-Tasman, 2000). WS attained great interest in cognitive neuroscience when it was proposed that this syndrome was a paradigm case of the modularity of mind by demonstrating independence of language from cognition (Bellugi et al., 1988). While this theory has been the subject of a far-ranging debate (Paterson et al., 1999), a number of studies have consistently demonstrated that a visuospatial constructive deficit lies at the core of the WS cognitive disturbance, forming a stable behavioral phenotype (Mervis et al., 2000). Of even greater importance may be the prospect that by understanding the neural mechanism of cognitive disturbance in WS, genetic factors underlying normal human visuospatial construction may be mapped, and basic information may be obtained about how genetic variation is transduced in the brain to produce cognitive disorders.

It is well established that the primate visual cortex is organized into two functionally specialized, hierarchically organized processing pathways, a ventral or "what" stream for object processing and a dorsal or "where" stream for spatial processing (Ungerleider and Mishkin, 1982). While these two streams show numerous complex interactions (Van Essen et al., 1992), and the division of labor between them is not clear cut, several authors (Atkinson et al., 2003; Galaburda et al., 2002; Nakamura et al., 2001; Paul et al., 2002) have hypothesized that the neural basis of the visuospatial constructive deficit in WS might lie in the dorsal stream. However, little evidence on the neural level has been obtained so far. Because the WS population exhibits, on average, mild to moderate mental retardation, functional neuroimaging studies are met with substantial confounds: participants with WS may be too impaired to fully cooperate; comparison groups of matched IQ may suffer from pathology as well; or, if the comparison group is of normal intelligence, then the differences between groups may be due to differences in IQ alone. In the present study, we addressed these confounds by recruiting an exceptional group of 13 individuals with genetically confirmed WS (Lowery et al., 1995) and classic-length 7q11.23 microdeletions but normal general intelligence. We reasoned that differences between these individuals (who had the same genes deleted as individuals with WS who have mental retardation) and IQ-matched individuals in the general population would likely be due to the core cognitive disturbance of WS and closely linked to the underlying genetic alteration rather than to more general factors associated with low IQ. This high-functioning group of individuals with WS was studied using functional and structural neuroimaging and compared to normal controls matched for age, sex, handedness, and estimated IQ (Table 1).

We tested the hypothesis of dorsal stream abnormality in WS with a series of fMRI experiments designed to access visual system function at several levels of the processing hierarchy. To assess the selectivity of our

*Correspondence: andreasml@nih.gov

Table 1. Demographics and Behavioral Data

	WS (n = 13)	Controls (n = 11)	p
Gender	6 M, 7 F	6 M, 5 F	
Age	28.3 ± 9.6	30.8 ± 7.6	NS
IQ	92.1 ± 9.6*, 85.4 ± 8.6**	96.8 ± 6.5	NS
Match accuracy	73.72 ± 16.32	81.58 ± 18.74	NS
Match reaction time	1478.04 ± 191.46	1559.16 ± 276.26	NS
Number of responses during match	37.98 ± 5.07	38.48 ± 3.43	NS
Square accuracy	56.73 ± 12.48	75.16 ± 15.64	<0.001
Square reaction time	1682.19 ± 457.32	2213.34 ± 615.87	<0.001
Number of responses during square	49.2 ± 7.48	42.45 ± 10.65	0.004

One individual with WS did not participate in the square completion task. All participants were right-handed. One control participant was African-American; the other participants in both groups were Caucasian, non-Hispanic. IQs were measured by the *two- and **four-subset forms of the Wechsler Abbreviated Scale of Intelligence (Wechsler, 1999) for participants with WS and a short form of the Wechsler Adult Intelligence Scale-Revised (Missar et al., 1994) for controls. Percent correct for the square completion task during the match and construction conditions, shown as mean ± standard deviation. Mean reaction time also shown in ms. NS, not significant.

findings, we tested not only for dorsal but also for ventral stream function, since some data from participants with WS who have mental retardation indicate early visual (Grice et al., 2003) or face processing (Mills et al., 2000) abnormalities.

Next, to identify underlying morphological abnormalities, participants were studied with high-resolution structural MRI. We wished to canvas the entire brain for significant morphological alterations without being constrained by anatomical landmarks. For this, we employed voxel-based morphometry (VBM), a widely used and validated (Good et al., 2002) method that can be sensitive to disease-related alterations that are not discernible using conventional MRI analysis (May et al., 1999) and that was recently applied to participants with WS who have mental retardation (Reiss et al., 2004). Pioneering work in Turner syndrome has demonstrated the feasibility of localizing regional structural alterations in the setting of haploinsufficiency using a combination of VBM and deletion mapping (Good et al., 2003).

Finally, since our results suggested a close link between structural and functional abnormalities, we employed path analysis to understand the functional interactions between visual brain regions in WS. This technique, widely applied in neuroimaging, takes into account anatomical constraints and functional interregional correlations to determine the influence of one brain region on another (McIntosh et al., 1994).

Using this hierarchical series of multimodal imaging experiments, we identified as a neural substrate of the visuospatial construction deficit in WS a circumscribed bilateral hypofunction in the dorsal visual stream that was attributable to impaired input from a directly adjacent region of reduced gray matter volume in the parietooccipital/intraparietal sulcus.

Results

Coordinates and statistics for all significant group differences are given in this section. Tables with significant within-group activations for each task can be found in the Supplemental Data at http://www.neuron.org/cgi/content/full/43/5/623/DC1.

Functional Activation Studies

Square Completion

In the first fMRI experiment, we presented participants with two monochromatic shapes whose borders were defined by a complex spatial arrangement of elementary geometric primitives. Participants either compared them (match condition; Figure 1A) or determined whether they could be assembled into a square (construction condition; Figure 1C). While object matching is a visuoperceptive task known to engage the ventral stream, the objects presented here were mainly defined by the relative orientation of elementary border features and were thus expected to activate the dorsal pathway as well. The construction condition, modeled after the classic block design task (Wechsler, 1997), additionally required visuospatial constructive function. In accordance with the a priori hypothesis, while both groups activated the ventral stream equally well, participants with WS showed a significant hypoactivation in dorsal stream areas in the match minus motor contrast (Figure 1B; Supplemental Table S1 at http://www.neuron.org/cgi/content/full/43/5/623/DC1). In the construction minus match comparison, designed to isolate visuospatial constructive function, normal controls activated the dorsal stream bilaterally, whereas participants with WS showed no significant activation (Supplemental Table S2 at http://www.neuron.org/cgi/content/full/43/5/623/DC1), again resulting in a significant dorsal stream hypoactivation on group comparison (Figure 1D). Although these findings were generally bilateral, the group by condition interaction reached stringent significance only in the left hemisphere for construction minus match ([x, y, z] coordinates −38, −52, 59, z score = 4.22) and the right for match minus motor (coordinates 23, −67, 49, z = 4.17) comparisons. No group differences were found in the ventral stream. To ensure that these observations were not due to problems with spatial normalization in individuals with WS, single-subject analyses were performed in native space. These confirmed the findings, demonstrating consistent hypofunction of dorsal but not ventral stream areas in individual participants with WS for each task and hemisphere (Table 2). No other task-related activation changes were observed. However, both groups deactivated the posterior superior temporal sulcus during both tasks, but participants with WS less

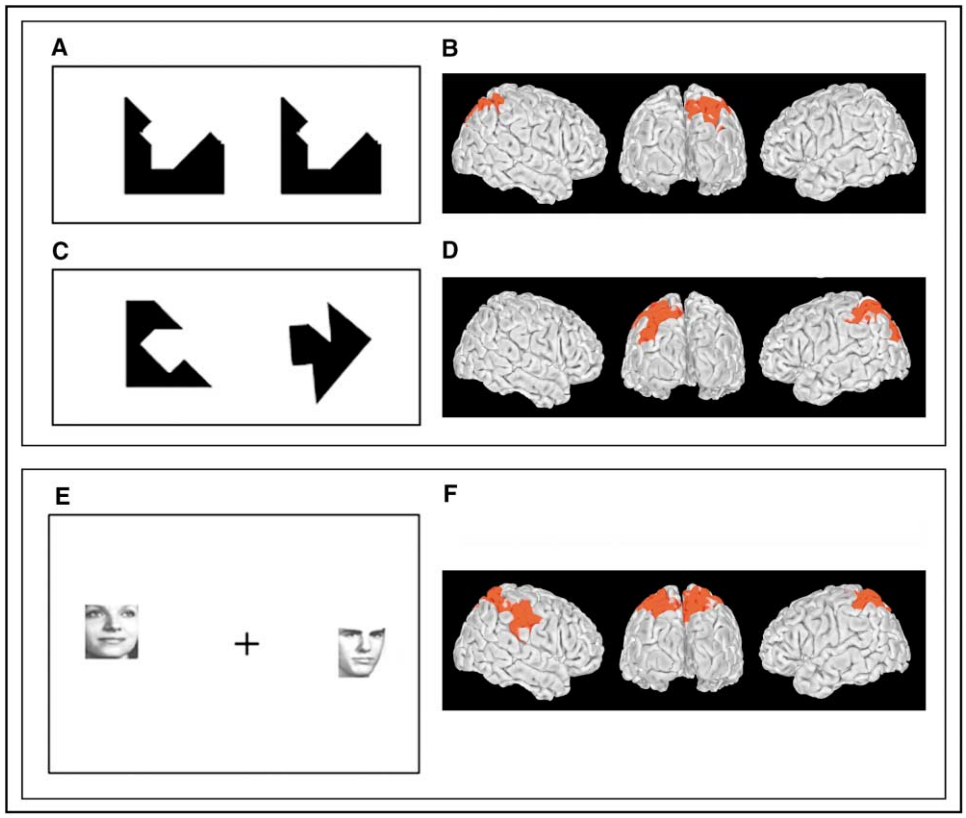

Figure 1. Stimuli and Significant Group Differences in Activation for the fMRI Tasks Used

(A) Example of stimuli for matching task.

(B) Significant hypoactivation in WS compared to controls in the match versus baseline contrast (matching task).

(C) Example of square completion stimuli.

(D) Significant hypoactivation in WS compared to controls in the construction versus match contrast (square completion task).

(E) Example of object versus location task stimuli. Both face (shown) and house stimuli were used.

(F) Significant hypoactivation in WS compared to controls in the location > object contrast (location versus object task). All activation difference maps are significant at $p < 0.05$ cluster level corrected for multiple comparisons (voxel threshold, $p < 0.001$).

so (significant at coordinates 49, −57, 15, z = 5.38; for match minus construction, −61, −34, 15, z = 3.55; for motor minus match, −57, −57, 11, z = 4.68). To exclude the possibility of an influence of performance, which was worse in participants with WS in the construction but not the matching task (Table 1), we used performance as a covariate in the statistical analysis. No correlations of brain activation with performance were found within groups for any condition, and no group by task interaction was found. Similarly, inclusion of age as a confounding covariate did not significantly alter the findings in any contrast.

Attention to Object or Location

In the final fMRI experiment, we used real-world stimuli (faces or houses) in a task of visual attention to either location or content (Figure 1E), previously shown to reliably and differentially delineate the dorsal and ventral streams, respectively (Haxby et al., 1991). This experi-

Table 2. Results of Single-Subject Analyses in Native Space for the Attention to Location and Square Completion Tasks

		WS*		Controls*		Statistics	
Task	Hemisphere	normal	abnormal	normal	abnormal	χ^2	p
Attention to location	L	2	11	9	2	10.6	0.001
	R	2	11	8	3	8.1	0.005
Match > control	L	3	9	9	2	7.4	0.006
	R	3	9	9	2	7.4	0.006
Construction > match	L	3	9	9	2	7.4	0.006
	R	2	10	9	2	9.8	0.002

*Number of participants with normal versus abnormal response. Significance levels are given for χ^2 tests on the number of abnormal and normal responses per group. One individual with WS did not participate in the square completion task. See the Experimental Procedures for methods.

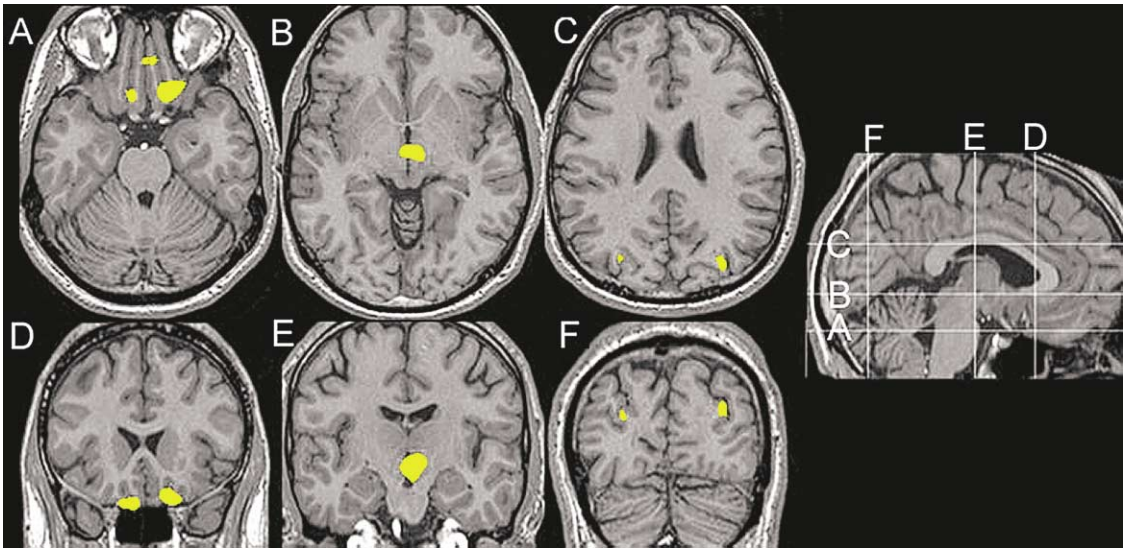

Figure 2. Results of Voxel-Based Morphometry Analysis of Structural MRIs

Areas of significant reduction in gray matter volume in WS, rendered on normalized single-subject MRI (thresholded at $t = 6.1$, $p < 0.05$, corrected voxel level), showing reductions in the occipitoparietal sulcus (C and F), the hypothalamic area (B and E), and orbitofrontally (A and D).

ment was expected to confirm findings from the square completion task and to provide further data on the processing of different classes of objects in the ventral stream. In accordance with the literature, normal controls activated the ventral stream during attention to object and the dorsal stream during attention to location (Supplemental Tables S3 and S4 at http://www.neuron.org/cgi/content/full/43/5/623/DC1). Participants with WS showed no difference from the normal controls in ventral stream activity, as confirmed by conjunction analysis showing extensive communal activation of the ventral stream in both groups (maxima at coordinates −15, −84, 8, z = 5.24, and 4, −65, 4, z = 5.14) as well as the cerebellum (coordinates 42, −53, −27, z = 5.95, and 34, −49, −30, z = 5.74). In contrast, a highly significant group by condition interaction demonstrated reduction in activation in the dorsal visual stream bilaterally in WS (coordinates −27, −60, 56, z = 5.23, and 23, −53, 48, z = 4.56), in a site very similar to that seen in the previous experiment (Figure 1F). Comparison of the ventral stream response to different object categories (faces and houses) indicated no difference between groups. This was confirmed with conjunction analyses showing highly significant joint activations of individuals with WS and controls in the fusiform face area for faces (coordinates 27, −46, −15, z = 5.52, and −34, −53, −15, z = 4.82) and in BA 18 and 19d for houses (coordinates 0, −84, 4, z = 6.16, and 57, −49, 4, z = 6.13). No regions were more active in WS in any contrast. Single-subject analyses in native space again confirmed these findings (Table 2).

Morphometric Studies

Our voxel-based approach, which incorporated a stringent statistical threshold, identified circumscribed symmetrical reductions in gray matter volume in WS in three regions (Figure 2 and Table 3): in the region of the dorsal occipitoparietal sulcus/vertical part of the intraparietal sulcus (PS), in the hypothalamic area around the third ventricle, and in the orbitofrontal region. No regions of increased gray matter volume in WS were observed.

Connectivity

Despite multiple cross-connections between its constituent regions (Ungerleider and Haxby, 1994), the primary organizational principle of the visual system is hierarchical, with information flowing in the dorsal stream from earlier, more inferior, to later, superior-anterior areas (Van Essen et al., 1992). Since our results showed a circumscribed structural alteration in region PS in immediate proximity to the hypofunction observed in our fMRI experiments (Figure 3), this suggested the hypothesis that our functional observations might be due to dysfunction of the structurally altered, more inferior PS region in WS, leading to hypoactivation in the remaining portion of the dorsal stream. To test this hypothesis directly, we turned to path analysis to model the interregional flow of information. We used data from the visual attention task and included the following nodes (Supplemental Table S5 at http://www.neuron.org/cgi/content/full/43/5/623/DC1): early visual areas, the most activated ventral stream region, the structurally changed PS region, and a dorsal stream location of pronounced between-group activation difference. The model was based on well-known anatomical constraints and was similar to previous path analyses of the visual system (McIntosh et al., 1994). We obtained a well-fitting model for both participant groups and then tested each path for significance of contribution to the overall fit (Figure 4). The only difference between groups was that the path from PS to the later dorsal stream region, while significant in controls, was not significant in WS (path coefficient 0.32, 95% confidence interval 0.13–0.52 in controls; in WS, path coefficient 0.03, confidence interval −0.17–0.22; see Figure 4). This finding was confirmed by stacked models statistics (significant difference between models χ^2-diff[1] = 101.8 − 97.3 = 4.5; $p < 0.02$).

Table 3. Reduced Gray Matter Volume in WS Participants in Voxel-Based Morphometry

Area	Talairach	z Score	p, Uncorrected
Occipito/intraparietal sulcus	−29, −79, 32	7.17	<0.001
	32, −75, 29	6.85	<0.001
Hypothalamus	−1, −13, −6	7.75	<0.001
Orbitofrontal cortex	17, 27, −26	8.19	<0.001
	−15, 27, −23	7.35	<0.001

Reported locations are those significant at a multiple comparison voxel threshold of $t = 6.1$ ($p < 0.05$, corrected).

Discussion

Both fMRI experiments showed consistent and circumscribed hypoactivation in the dorsal visual stream in our sample of high-functioning participants with WS. Our finding of normal ventral stream activation during both experiments in participants with WS supported the a priori hypothesis not only of the presence but also of the relative specificity of dorsal stream dysfunction, at least in the context of our experimental procedures. The findings from the attention to location task, the match condition, and the construction condition were strikingly similar in their extent and locale, both in tasks where participants with WS performed normally and in those in which they performed worse than controls. This suggests that these findings reflect a consistent dysfunction in WS and were not attributable to performance differences. Rather, our interpretation of these findings is that this hypoactivation reflects a persistent functional deficit in WS that may become rate limiting (with deteriorating performance) when higher demands are placed on the dorsal stream during construction.

Of the regions of reduced gray matter volume identified in WS, only PS lies in visual cortex. A reduction of gray matter density in a very similar locale was also observed recently in persons with WS and mental retardation (Reiss et al., 2004), and abnormal gyrification in the parietal lobule was found by Schmitt et al. (2002). While the precise change underlying the observation in PS (such as a reduction of adjacent parietal or occipital volume or abnormal folding) remains to be demonstrated, PS was clearly located anatomically in the dorsal stream and situated directly adjacent to the region of hypofunction in WS (Figure 3), suggesting a structural-functional connection. This is supported by functional neuroimaging studies that confirm a role of PS in the dorsal stream (Orban et al., 1999) and suggest as possible homologs monkey areas V6 and LIP, both of which contain location-sensitive neurons (Simon et al., 2002). Specifically, our data suggested deficient input from PS into the later dorsal stream as a mechanism for the consistently observed hypoactivity in these regions. We tested this hypothesis directly using path analysis, which showed that our functional data could be accounted for by an absence of the functional path from PS to the later dorsal stream in participants with WS, confirming the critical functional role of decreased input from PS. This proposed mechanism might also explain otherwise puzzling findings of unimpaired visual motion detection in WS (Jordan et al., 2002), because moving stimuli could reach the dorsal stream via area MT in the temporal lobe, circumventing PS, further illustrating the complexity of the interactions existing between the visual processing domains.

It is interesting to note that the BOLD signal detected hypofunction not directly within PS itself, but in regions immediately adjacent to it (Figure 3). The fact that our data indicate a structural alteration in PS that results in

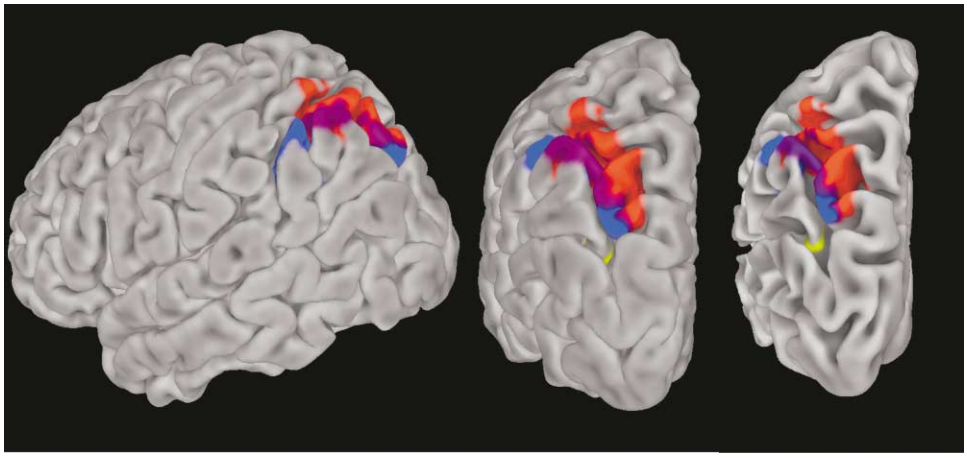

Figure 3. Spatial Relationship between Structurally and Functionally Abnormal Areas in WS

Spatial relationship between structurally altered area (yellow), hypoactivation during attention to location task (red), and square completion versus matching task (blue) in participants with WS compared to controls. Overlap regions are shown in purple. Statistics as described for separate analyses. Shown on lateral (left image) and posterior (middle image) view of left cortical reference surface. (Right) Posterior view of white matter surface border reconstruction, showing VBM finding in the sulcus.

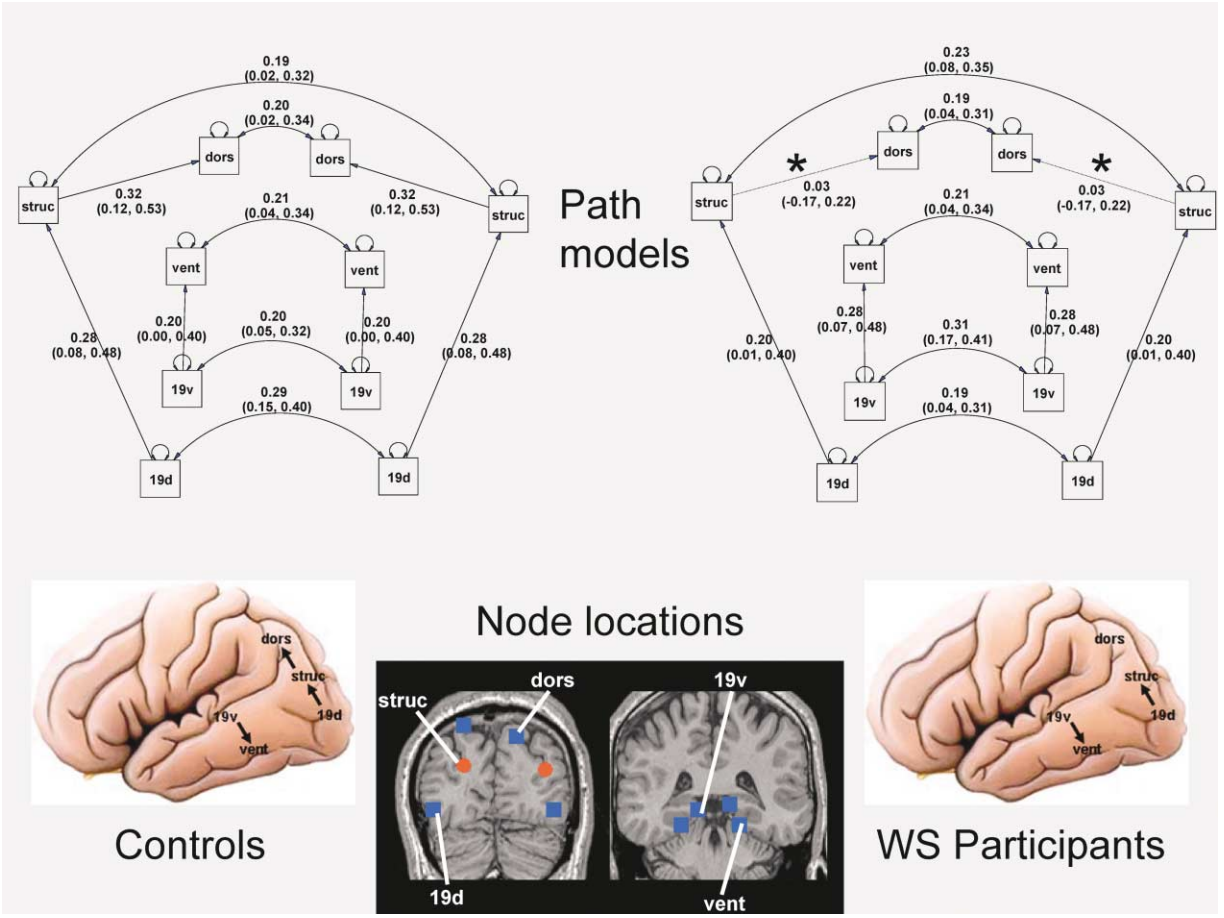

Figure 4. Results of Path Analysis of fMRI Data from the Object versus Location Task

The only significant difference between control (left) and WS participant (right) models is the lack of a path from the structurally altered area into the dorsal stream (starred), as shown in schematic drawings under the path models. (Middle) Location of modeled regions, shown on representative normal MRI. Structurally altered area is shown in red.

reduced flow of activation into the later dorsal stream supports preclinical evidence (Logothetis et al., 2001; Sokoloff, 1977) that hemodynamic (e.g., fMRI) responses are driven significantly by regional synaptic activity (reflecting input into an area) rather than by spiking activity of the local neurons themselves.

With respect to the debate about the modularity of mind, our data suggest one mechanism by which visuospatial cognition could be selectively impaired in WS—that is, because this impairment is due to hypofunction consequent to a localized structural-functional abnormality in a system which is itself highly modular and hierarchical in design. Conceivably, the impact of either less or differently localized pathology would not have been as relatively modular in this neuropsychological sense. Designed to assess the visual system, our functional data do not speak to other domains, where the neural pathomechanism and the cognitive result may be different. Given the dynamics of brain development, the route by which this deficit is arrived at is likely complex. Other functional alterations and possible compensatory mechanisms, especially in the developing brain and outside the visual system explored here, remain to be elucidated. In this context, our observation of reduced deactivation of the posterior superior temporal gyrus during both visual tasks in WS might be of interest. Because many cognitive tasks "deactivate" this region, it is widely assumed to be part of the "baseline state" (Gusnard and Raichle, 2001), and findings there have been dismissed as nonspecific. However, since it has been proposed that the baseline state reflects ongoing conceptual processing or social cognition (Binder et al., 1999), our observation might also indicate relatively increased task-unrelated activity in these domains in WS, suggesting further study.

Unlike our PS finding, less agreement exists between our other morphometric findings and previous studies of the brain morphology in participants with WS and mental retardation (Reiss et al., 2000, 2004; Schmitt et al., 2001), and they must therefore be viewed with caution. In general, while recruitment of an exceptional group of normal-intelligence participants with WS enabled an incisive study of cognitive function, the atypical nature of this sample also means that further functional and structural alterations might emerge in the general (lower functioning) WS population. However, the structural alterations found in the hypothalamic and orbitofrontal regions may point to pathophysiological mecha-

nisms underlying aspects of WS outside the cognitive deficit in visuospatial construction. The orbitofrontal cortex is known to be involved in regulating motivational, reward, and emotional aspects of social cognition (Adolphs, 2001). It is possible that dysfunction in this area might underlie the known overfriendliness and gregariousness observed in WS. Unlike the present results, Reiss et al. (2004) found increases in density in the orbitofrontal cortex, possibly because of differences in participant selection (participants with WS with normal intelligence or with mental retardation, controls matched or unmatched for IQ) or methodology (in that study only linear normalization but no shape adjustment was performed; thus, the observations in orbitofrontal cortex might reflect global shape differences). Further work is clearly needed to elucidate the contribution of this region to the WS phenotype.

Hormonal disturbances, including diabetes, thyroid dysfunction suggestive of hypothalamic hypothyroidism (Cammareri et al., 1999), and hypercalcemia, are found in WS, but their mechanism is not clearly understood. Abnormalities in the hypothalamus, as observed here, should prompt an investigation of possible central contributions to these often problematic aspects of everyday care for individuals with WS.

Our finding of localized and linked structural and functional dorsal stream abnormalities in WS defines a systems-level phenotype that should help inquiries into the underlying molecular mechanism, especially given the lack of murine models of visuospatial construction. While inconsistencies among studies remain, promising candidate genes include *LIM-kinase 1*, implicated by linkage in the genesis of the visuospatial constructive deficit (Frangiskakis et al., 1996), *CYLN2* (Hoogenraad et al., 2002), and *GTF2I* (Morris et al., 2003), recently found to be involved in neuronal maturation (Danoff et al., 2004). Neuroimaging studies of individuals with partial deletions (Frangiskakis et al., 1996; Morris et al., 2003) would be of special interest in narrowing down the search for the gene(s) involved in deficient visuospatial construction.

Experimental Procedures

Studied Populations

Participants with WS were identified from a large sample of adults with WS who had previously participated in behavioral studies conducted by C.B.M. Participants were selected because their IQs were within the normal range for the general population. Exclusionary criteria were chronological age >50 years (one individual excluded) or current treatment with psychotropic medication (one individual excluded). Of those identified, all but three decided to participate in this study. For the present study, IQ was ascertained using the two- and four-subset forms of the Wechsler Abbreviated Scale of Intelligence (Wechsler, 1999) for participants with WS and a short form of the Wechsler Adult Intelligence Scale-Revised (Missar et al., 1994) for controls. Control subjects were recruited by advertisement and matched groupwise for IQ, gender, and age. Matching was accomplished using the two-subtest form for participants with WS, which consisted of the Vocabulary and Matrix Reasoning subtests, to avoid a confound, because visuospatial constructive problems artificially lower IQ in the four-subtest form and would thus have resulted in a biased match on general IQ. WASI two-subtest IQs ranged from 77 to 112, placing all participants with WS within the normal IQ range for the general population and the top 15% of the IQ distribution for WS. All participants with WS had confirmed classic hemideletions on chromosome 7q11.23 and exhibited classic WS physical features. Demographic data are given in Table 1. All participants with WS and all but one of the control participants were Caucasian, non-Hispanic. Informed consent was obtained from all participants after the nature and possible consequences of the studies were explained in accordance with the NIMH IRB. All participants were reimbursed for their participation according to NIH guidelines.

Functional Neuroimaging

Blood oxygen level-dependent T2*-weighted gradient-echo echo-planar images (TR = 3 s, TE = 30 ms, FOV = 24 cm, 90° flip, 64 × 64 matrix, 36 contiguous and sequential slices, voxel size 3.75 × 3.75 × 4 mm) were acquired on a 3-T General Electric Signa scanner with whole-head coil (IGC-Medical Advances, Milwaukee, WI). Stimuli were presented and responses were registered using in-house software and a binocular fiber-optic goggle system (Avotec, Stuart, FL). Responses were with the right thumb.

Functional Image Analysis

All analysis steps were performed using SPM99 (http://www.fil.ion.ucl.ac.uk/spm/spm99.html). After registration and slice timing correction, for group analysis, images were normalized to a template specifically constructed for the study population from 12 control and 12 WS normalized mean EPI images. Images were smoothed with a 10 mm (isotropic) Gaussian filter and analyzed using the general linear model. Task conditions were modeled as epochs convolved with a generic hemodynamic function. Drift and other low-frequency effects were reduced by global scaling and high-pass filtering. Resulting statistical maps were compared at the second level using Student's t tests for random-effects group statistics, thresholded at $p < 0.001$ (uncorrected), and then corrected for multiple comparisons at the cluster level ($p < 0.05$) (Friston et al., 1996). For single-subject analyses, data were analyzed as described before, but in native space and overlaid onto cortical surface representations constructed from the individual participant's high-resolution structural images. Single-subject results were classified as normal if any activation in ventral respectively dorsal stream areas was found at a liberal $p < 0.001$ (uncorrected) threshold and as abnormal otherwise. Coordinates are reported in mm according to the Talairach (Talairach and Tournoux, 1988) system.

Square Completion Task

Each 360 s scan (three scans per subject) consisted of a pseudorandomized and balanced sequence of three conditions in blocks of 18 s with 2.8 s intertrial interval: square, match, and motor control. The task was self-paced with a maximum time of 7 s per stimulus pair. Stimuli consisting of pairs of black shapes with a boundary of elementary line segments were presented to the left and right of a fixation cross, with task instruction present throughout the block under the cross. In motor control, each presentation was of a matching pair, and the same button was pressed. In the matching task, a shape was presented with either an identical copy or its mirror image. Participants pressed one of two buttons depending on whether or not they were the same. In square completion, participants were instructed to determine whether or not the two shapes could be fit together to make a square without flipping them over. Performance data are summarized in Table 1.

Attention Task

Each of three scans of 588 s consisted of 9 s blocks with 2.4 s intertrial interval in two conditions: location or object. Stimuli consisted of pictures of faces or houses or noise (matched spatial frequency). On each trial, a stimulus appeared first on the left and then on the right of the fixation cross at one of five vertical positions for 1.2 s. In the object condition, participants pressed one of two buttons depending on whether the two pictures were the same or different. In the location condition, the instruction was to respond based on whether the left and right pictures were at the same vertical position relative to the fixation cross. Five rest blocks were spaced evenly throughout the task.

Structural Neuroimaging

Six axially acquired T1-weighted structural MRIs (TE = 5.2 ms, TR = 12 ms, FOV = 24 mm, resolution 0.94 × 0.94 × 1.2 mm) were registered and averaged. MRI scans were processed using the optimized VBM protocol (Good et al., 2001). To optimize gray-white matter discrimination, group-specific templates were constructed for WS and normal controls and used for segmentation. For spatial normalization, all data were aligned to the average of these two templates to avoid biasing the normalization toward one of the compared groups. After 12-parameter affine mapping, nonlinear normalization using an optimal linear combination of 4 × 5 × 4 spatial basis function was performed. Jacobian-modulated gray matter maps were smoothed with a 10 mm (isotropic) Gaussian filter. All structural processing and analyses were performed using SPM2 (http://www.fil.ion.ucl.ac.uk/spm/spm2.html). Random-effects group statistics were by Student's t tests on the second level. Resulting statistical maps were corrected for multiple comparisons by thresholding for significance by voxel intensity at the $p < 0.05$ (corrected) level.

Path Analysis

Our methods for model fitting, selection, and evaluation have been previously described (Glabus et al., 2003). Briefly, models were fitted from covariance matrices using the software package Mx (http://www.vcu.edu/mx/). Path coefficients were constrained to be symmetric. Interhemispheric connections were included between homologous areas only. Residual variance was fixed at 0.65 at each node. The final model only included path coefficients that were significant in healthy controls. The final model fit both groups very well [χ^2 (94, 16) = 94.0; p = 0.48; AIX = −94, 0; RSMEA = 0.022]. After good fit was established, each path was separately tested for significance, showing that the only difference between groups was that the path from the occipitoparietal sulcus to the later dorsal stream was significant in participants in the control group but not in participants with WS. This finding was confirmed using a stacked models approach comparing a model in which this path only was allowed to be different between groups with a model in which all paths were restricted to be equal, yielding a significant difference.

Acknowledgments

We thank our participants and their families; John Pani for suggesting the use of the square completion task; Terry Goldberg for providing a number of the IQ scores for healthy controls; Venkata Mattay for MRI expertise; and John Holt, Neha Dixit, and Aaron Bonner-Jackson for research assistance. This work was supported by DHHS/NIH/NIMH/IRP and NINDS grant #NS35102 (C.B.M., principal investigator).

Received: April 30, 2004
Revised: June 24, 2004
Accepted: August 4, 2004
Published: September 1, 2004

References

Adolphs, R. (2001). The neurobiology of social cognition. Curr. Opin. Neurobiol. *11*, 231–239.

Atkinson, J., Braddick, O., Anker, S., Curran, W., Andrew, R., Wattam-Bell, J., and Braddick, F. (2003). Neurobiological models of visuospatial cognition in children with Williams syndrome: measures of dorsal-stream and frontal function. Dev. Neuropsychol. *23*, 139–172.

Bellugi, U., Sabo, H., and Vaid, J. (1988). Dissociation between language and cognitive functions in Williams syndrome. In Language Development in Exceptional Circumstances, D.V.M. Bishop and K. Mogford-Bevan, eds. (Edinburgh/New York: Churchill Livingstone), pp. 177–189.

Binder, J.R., Frost, J.A., Hammeke, T.A., Bellgowan, P.S., Rao, S.M., and Cox, R.W. (1999). Conceptual processing during the conscious resting state. A functional MRI study. J. Cogn. Neurosci. *11*, 80–95.

Cammareri, V., Vignati, G., Nocera, G., Beck-Peccoz, P., and Persani, L. (1999). Thyroid hemiagenesis and elevated thyrotropin levels in a child with Williams syndrome. Am. J. Med. Genet. *85*, 491–494.

Danoff, S.K., Taylor, H.E., Blackshaw, S., and Desiderio, S. (2004). TFII-I, a candidate gene for Williams syndrome cognitive profile: parallels between regional expression in mouse brain and human phenotype. Neuroscience *123*, 931–938.

Frangiskakis, J.M., Ewart, A.K., Morris, C.A., Mervis, C.B., Bertrand, J., Robinson, B.F., Klein, B.P., Ensing, G.J., Everett, L.A., Green, E.D., et al. (1996). LIM-kinase1 hemizygosity implicated in impaired visuospatial constructive cognition. Cell *86*, 59–69.

Friston, K.J., Holmes, A., Poline, J.B., Price, C.J., and Frith, C.D. (1996). Detecting activations in PET and fMRI: levels of inference and power. Neuroimage *4*, 223–235.

Galaburda, A.M., Holinger, D.P., Bellugi, U., and Sherman, G.F. (2002). Williams syndrome: neuronal size and neuronal-packing density in primary visual cortex. Arch. Neurol. *59*, 1461–1467.

Glabus, M.F., Horwitz, B., Holt, J.L., Kohn, P.D., Gerton, B.K., Callicott, J.H., Meyer-Lindenberg, A., and Berman, K.F. (2003). Interindividual differences in functional interactions among prefrontal, parietal and parahippocampal regions during working memory. Cereb. Cortex *13*, 1352–1361.

Good, C.D., Johnsrude, I.S., Ashburner, J., Henson, R.N., Friston, K.J., and Frackowiak, R.S. (2001). A voxel-based morphometric study of ageing in 465 normal adult human brains. Neuroimage *14*, 21–36.

Good, C.D., Scahill, R.I., Fox, N.C., Ashburner, J., Friston, K.J., Chan, D., Crum, W.R., Rossor, M.N., and Frackowiak, R.S. (2002). Automatic differentiation of anatomical patterns in the human brain: validation with studies of degenerative dementias. Neuroimage *17*, 29–46.

Good, C.D., Lawrence, K., Thomas, N.S., Price, C.J., Ashburner, J., Friston, K.J., Frackowiak, R.S., Oreland, L., and Skuse, D.H. (2003). Dosage-sensitive X-linked locus influences the development of amygdala and orbitofrontal cortex, and fear recognition in humans. Brain *126*, 2431–2446.

Grice, S.J., Haan, M.D., Halit, H., Johnson, M.H., Csibra, G., Grant, J., and Karmiloff-Smith, A. (2003). ERP abnormalities of illusory contour perception in Williams syndrome. Neuroreport *14*, 1773–1777.

Gusnard, D.A., and Raichle, M.E. (2001). Searching for a baseline: functional imaging and the resting human brain. Nat. Rev. Neurosci. *2*, 685–694.

Haxby, J.V., Grady, C.L., Horwitz, B., Ungerleider, L.G., Mishkin, M., Carson, R.E., Herscovitch, P., Schapiro, M.B., and Rapoport, S.I. (1991). Dissociation of object and spatial visual processing pathways in human extrastriate cortex. Proc. Natl. Acad. Sci. USA *88*, 1621–1625.

Hillier, L.W., Fulton, R.S., Fulton, L.A., Graves, T.A., Pepin, K.H., Wagner-McPherson, C., Layman, D., Maas, J., Jaeger, S., Walker, R., et al. (2003). The DNA sequence of human chromosome 7. Nature *424*, 157–164.

Hoogenraad, C.C., Koekkoek, B., Akhmanova, A., Krugers, H., Dortland, B., Miedema, M., van Alphen, A., Kistler, W.M., Jaegle, M., Koutsourakis, M., et al. (2002). Targeted mutation of Cyln2 in the Williams syndrome critical region links CLIP-115 haploinsufficiency to neurodevelopmental abnormalities in mice. Nat. Genet. *32*, 116–127.

Jordan, H., Reiss, J.E., Hoffman, J.E., and Landau, B. (2002). Intact perception of biological motion in the face of profound spatial deficits: Williams syndrome. Psychol. Sci. *13*, 162–167.

Logothetis, N.K., Pauls, J., Augath, M., Trinath, T., and Oeltermann, A. (2001). Neurophysiological investigation of the basis of the fMRI signal. Nature *412*, 150–157.

Lowery, M.C., Morris, C.A., Ewart, A., Brothman, L.J., Zhu, X.L., Leonard, C.O., Carey, J.C., Keating, M., and Brothman, A.R. (1995). Strong correlation of elastin deletions, detected by FISH, with Williams syndrome: evaluation of 235 patients. Am. J. Hum. Genet. *57*, 49–53.

May, A., Ashburner, J., Buchel, C., McGonigle, D.J., Friston, K.J., Frackowiak, R.S., and Goadsby, P.J. (1999). Correlation between

structural and functional changes in brain in an idiopathic headache syndrome. Nat. Med. *5*, 836–838.

McIntosh, A.R., Grady, C.L., Ungerleider, L.G., Haxby, J.V., Rapoport, S.I., and Horwitz, B. (1994). Network analysis of cortical visual pathways mapped with PET. J. Neurosci. *14*, 655–666.

Mervis, C.B., and Klein-Tasman, B.P. (2000). Williams syndrome: Cognition, personality, and adaptive behavior. Ment. Retard. Dev. Disabil. Res. Rev. *6*, 148–158.

Mervis, C.B., Robinson, B.F., Bertrand, J., Morris, C.A., Klein-Tasman, B.P., and Armstrong, S.C. (2000). The Williams syndrome cognitive profile. Brain Cogn. *44*, 604–628.

Mills, D.L., Alvarez, T.D., St. George, M., Appelbaum, L.G., Bellugi, U., and Neville, H. (2000). III. Electrophysiological studies of face processing in Williams syndrome. J. Cogn. Neurosci. Suppl. *12*, 47–64.

Missar, C.D., Gold, J.M., and Goldberg, T.E. (1994). WAIS-R short forms in chronic schizophrenia. Schizophr. Res. *12*, 247–250.

Morris, C.A., Mervis, C.B., Hobart, H.H., Gregg, R.G., Bertrand, J., Ensing, G.J., Sommer, A., Moore, C.A., Hopkin, R.J., Spallone, P.A., et al. (2003). GTF2I hemizygosity implicated in mental retardation in Williams syndrome: Genotype-phenotype analysis of five families with deletions in the Williams syndrome region. Am. J. Med. Genet. *123A*, 45–59.

Nakamura, M., Watanabe, K., Matsumoto, A., Yamanaka, T., Kumagai, T., Miyazaki, S., Matsushima, M., and Mita, K. (2001). Williams syndrome and deficiency in visuospatial recognition. Dev. Med. Child Neurol. *43*, 617–621.

Orban, G.A., Sunaert, S., Todd, J.T., Van Hecke, P., and Marchal, G. (1999). Human cortical regions involved in extracting depth from motion. Neuron *24*, 929–940.

Paterson, S.J., Brown, J.H., Gsodl, M.K., Johnson, M.H., and Karmiloff-Smith, A. (1999). Cognitive modularity and genetic disorders. Science *286*, 2355–2358.

Paul, B.M., Stiles, J., Passarotti, A., Bavar, N., and Bellugi, U. (2002). Face and place processing in Williams syndrome: evidence for a dorsal-ventral dissociation. Neuroreport *13*, 1115–1119.

Reiss, A.L., Eliez, S., Schmitt, J.E., Straus, E., Lai, Z., Jones, W., and Bellugi, U. (2000). IV. Neuroanatomy of Williams syndrome: a high-resolution MRI study. J. Cogn. Neurosci. Suppl. *12*, 65–73.

Reiss, A.L., Eckert, M.A., Rose, F.E., Karchemskiy, A., Kesler, S., Chang, M., Reynolds, M.F., Kwon, H., and Galaburda, A. (2004). An experiment of nature: brain anatomy parallels cognition and behavior in Williams syndrome. J. Neurosci. *24*, 5009–5015.

Schmitt, J.E., Eliez, S., Bellugi, U., and Reiss, A.L. (2001). Analysis of cerebral shape in Williams syndrome. Arch. Neurol. *58*, 283–287.

Schmitt, J.E., Watts, K., Eliez, S., Bellugi, U., Galaburda, A.M., and Reiss, A.L. (2002). Increased gyrification in Williams syndrome: evidence using 3D MRI methods. Dev. Med. Child Neurol. *44*, 292–295.

Simon, O., Mangin, J.F., Cohen, L., Le Bihan, D., and Dehaene, S. (2002). Topographical layout of hand, eye, calculation, and language-related areas in the human parietal lobe. Neuron *33*, 475–487.

Sokoloff, L. (1977). Relation between physiological function and energy metabolism in the central nervous system. J. Neurochem. *29*, 13–26.

Talairach, J., and Tournoux, P. (1988). Co-Planar Stereotaxic Atlas of the Human Brain: 3-Dimensional Proportional System: An Approach to Cerebral Imaging (Stuttgart, Germany/New York: Thieme Medical Publishers).

Ungerleider, L.G., and Haxby, J.V. (1994). 'What' and 'where' in the human brain. Curr. Opin. Neurobiol. *4*, 157–165.

Ungerleider, L.G., and Mishkin, M. (1982). Two cortical visual systems. In Analysis of Visual Behavior, D.J. Ingle, D.J. Goodale, and R.J.W. Mansfield, eds. (Cambridge, MA: The MIT Press), pp. 549–586.

Van Essen, D.C., Anderson, C.H., and Felleman, D.J. (1992). Information processing in the primate visual system: an integrated systems perspective. Science *255*, 419–423.

Wechsler, D. (1997). Wechsler Adult Intelligence Scale, Third Edition (San Antonio, TX: The Psychological Corporation).

Wechsler, D. (1999). Wechsler Abbreviated Scale of Intelligence (San Antonio, TX: The Psychological Corporation).